Applied Catalysis B: Environmental 232 (2018) 60–68

Contents lists available at ScienceDirect

Applied Catalysis B: Environmental

journal homepage: www.elsevier.com/locate/apcatb

Electrochemical promotion of nanodispersed Ru-Co catalysts for the hydrogenation of CO_2

A. Kotsiras[a], I. Kalaitzidou[a], D. Grigoriou[a], A. Symillidis[a], M. Makri[a], A. Katsaounis[a], C.G. Vayenas[a,b,*]

[a] Department of Chemical Engineering, Caratheodory 1 St., University of Patras, GR-26504 Patras, Greece
[b] Academy of Athens, Panepistimiou 28 Ave., GR-10679 Athens, Greece

ARTICLE INFO

Keywords:
Electrochemical promotion
EPOC
NEMCA effect
CO_2 hydrogenation
Dispersed catalyst

ABSTRACT

Electrochemical promotion of the CO_2 hydrogenation to CH_4 and CO on a nanodispersed Ru-Co catalyst has been achieved via slurry deposition of the nanodispersed catalyst on an interlayer Ru film deposited on a BZY ($BaZr_{0.85}Y_{0.15}O_3$) proton conducting solid electrolyte disc. The effect of current is nonFaradaic, with Faradaic efficiency values as high as 60 and leads to a reversible variation of the selectivity to CH_4 between 16% and 41%. Due to thermal spillover of protons on the Ru-Co catalyst surface, the open circuit selectivity to CO is quite high, i.e. up to 84% and similar values are obtained via negative potential application, i.e. proton supply to the Ru catalyst film deposited on BZY before the deposition of the nanodispersed catalyst. These results underline the similarity between electrochemical promotion and metal support interactions when using proton conducting supports. They also show the usefulness of electrochemical promotion for mechanistic investigations. The electrochemical promotion of nanodispersed catalysts is a promising step for the practical utilization of electrochemical promotion.

1. Introduction

The hydrogenation of CO_2 to hydrocarbons or alcohols is among the most important chemical conversions of CO_2 not only for the production of renewable fuels but also as a possible means for decreasing the overall CO_2 emissions [1–5]. Several metals (e.g. Cu, Pt, Rh, Pd, Ru, Fe, Co, Ni) have been investigated as catalysts on a variety of supports (e.g. Nb_2O_5, ZrO_2, Al_2O_3, SiO_2) with several alkali-based promoters. Work in this area has been reviewed recently [1,3–9]. The hydrogenation of CO_2 on Ru, which is known to give only CH_4 and CO as products, has received considerable attention in recent years [8–11].

The dissociative adsorption of CO_2 to CO and O has been suggested in the past to be the initial step reaction for CO_2 hydrogenation. According to this series mechanism CO, is further decomposed to C and O followed by the hydrogenation of C to CH_4. An alternative parallel mechanism has been also proposed [12–16] introducing the formation of formate at the metal-support interface which acts as an intermediate product for methane and CO production.

In order to reduce the catalyst costs, many research groups have focused their attention on alternative low cost catalysts. Cobalt based catalysts supported on high surface materials such as γ-Al_2O_3, SiO_2, TiO_2, CeO_2, and ZrO_2 were proposed in the literature [17–19].

A parallel approach to classical chemical promotion is the electrochemical promotion of catalysis (EPOC) or the non-faradaic electrochemical modification of catalytic activity (NEMCA) effect [20–36] which can be used to promote metal-catalyst films simultaneously acting as electrodes, deposited on solid electrolyte supports, such as yttria-stabilized-ZrO_2 (YSZ, an O^{2-} conductor) or β''-Al_2O_3 (a Na^+ or K^+ conductor), or mixed ionic-electronic conductors such as TiO_2 or CeO_2. Upon application of a change, ΔU_{WR}, to the electrical potential, U_{WR}, of the catalyst (working electrode) with respect to a reference electrode these backspillover species, accompanied by their compensating charge in the metal, migrate to the metal-gas interface, creating an overall neutral double layer, termed the effective double layer. This ion backspillover causes the catalyst work function, Φ, to change by $\Delta\Phi = e\Delta U_{WR}$ and accordingly the chemisorptive bond strengths of the reactants and intermediates are modified [20–36]. Thus, both catalytic activity and selectivity are affected in a pronounced, reversible, and, to some extent, predictable manner [20–36]. The close connection between EPOC, classical chemical promotion and metal support interaction (MSI) with ionically conducting supports has been established by a variety of techniques [20,21,25,29–37].

There are two parameters that are commonly used to quantify the magnitude of EPOC [20]:

* Corresponding author at: Department of Chemical Engineering, Caratheodory 1 St., University of Patras, GR-26504 Patras, Greece.
E-mail address: cgvayenas@upatras.gr (C.G. Vayenas).

https://doi.org/10.1016/j.apcatb.2018.03.031
Received 13 November 2017; Received in revised form 27 February 2018; Accepted 9 March 2018
Available online 10 March 2018
0926-3373/

the rate enhancement ratio, ρ, defined by Eq. (1):

$$\rho = \frac{r}{r_o} \tag{1}$$

in which r is the electropromoted catalytic rate and r_o is the unpromoted rate (i.e. the open-circuit catalytic rate), and

the apparent Faradaic efficiency, Λ, defined by Eq. (2):

$$\Lambda = \frac{\Delta r_{catalytic}}{(I/F)} \tag{2}$$

where $\Delta r_{catalytic}$ is the current- or potential-induced observed change in catalytic rate in (g-eq/s) and I is the applied current. In the present case, accounting for the stoichiometry of the methanation and of the reverse water-gas shift (RWGS) reactions, i.e.

$$CO_2 + 4H_2 \rightarrow CH_4 + 2H_2O \tag{3}$$

$$CO_2 + H_2 \rightarrow CO + H_2O \tag{4}$$

one obtains

$$\Lambda_{CH_4} = \frac{8\Delta r_{CH_4}}{(I/F)} \tag{5}$$

$$\Lambda_{CO} = \frac{\Delta r_{CO}}{(I/F)} \tag{6}$$

where r_{CH4} is in mol CH_4/s and r_{CO} is in mol CO/s

A reaction is termed electrophobic (or nucleophilic) when the rate increases with increasing catalyst potential ($\partial r/\partial U_{WR} > 0$), electrophilic when the rate decreases with increasing catalyst potential ($\partial r/\partial U_{WR} < 0$), volcano-type when the reaction rate exhibits a maximum with varying potential, and inverted volcano when the rate goes through a minimum with varying potential [20,38–41]. The electrochemical promotion of CO_2 has been studied in the past on Ru [42–46] catalyst film electrodes deposited on YSZ (8%mol Y_2O_3-ZrO_2) [42,43,46], $BaZrO_{0.85}Y_{0.15}O_3$ (BZY), a H^+ conductor [45,46], β″-Al_2O_3-K^+ conductor [43,46] and β″-Al_2O_3-Na^+ ionic conductor [44,46]. In general, in all these studies the rate of methanation was found to exhibit electrophobic behavior, whereas the rate of CO formation via the RWGS reaction was found to follow electrophilic behavior.

There have been so far only a couple of studies exploring the electrochemical promotion of industrial or promoted dispersed catalysts. The more recent one was reported by Kambolis et al [47] and discusses the electrochemical promotion of propane oxidation on Pt nanoparticles and the older one was presented by Yiokari et al [48] and describes the electropromotion of ammonia synthesis using a state of the art, fully promoted, industrial Fe-based catalyst. Zhou and coworkers [49,50] have recently developed some very interesting self-sustained electrochemical promotion catalysts in which the catalyst consists of microscopic anodic, cathodic, ion conducting (YSZ) and electronically conducting (Ni-Cu) phases. In parallel to the above studies, there are studies addressing the similarity of electrochemical promotion and metal-support interaction for the case of oxygen ion supports [36,51–53]. It was observed that the TOF values of the dispersed Rh/YSZ catalyst fall between those of unpromoted and electropromoted Rh/YSZ electrochemical catalyst. This implies that the dispersed catalysts are, to some extent, partially promoted due to the thermal migration of the promoting O^{2-} species from the support (YSZ) to the metal particles surface.

In the present study, we explore the effect of electrochemical promotion for CO_2 hydrogenation using a nanodispersed catalyst (2%Ru-15%Co supported on BZY powder) deposited on a porous Ru catalyst film supported on a $BaZr_{0.85}Y_{0.15}O_3$ +1wt %NiO (BZY) proton conductor disc (Fig. 1). During the last two decades, new materials with proton conductivity have been developed and proposed mainly for fuel cell applications [54–59]. One of them is BZY prepared by NorECs AS and used in this study, which is shown to exhibit excellent properties for carrying out electrochemical promotion studies [55]. We have thus investigated the effect of catalyst loading and catalyst potential on the catalytic activity and selectivity of the CO_2 methanation and the RWGS reactions at temperatures 350° to 450 °C and ambient pressure. The present study is the first one exploring the similarities between electrochemical promotion and metal-support interactions for the case of a proton conducting support during a hydrogenation reaction. In addition, the present study is the first discussing the electrochemical promotion of a dispersed Ru-Co catalyst.

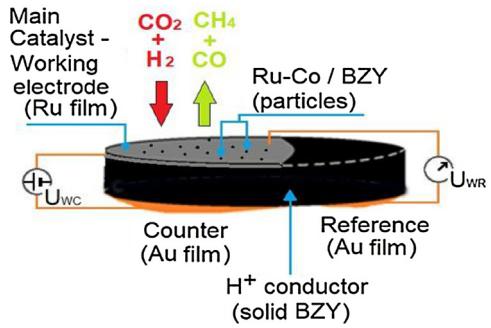

Fig. 1. Schematic of the BZY support disc and its three electrodes, one serving as the catalyst. Also shown schematically is the catalyst preparation procedure.

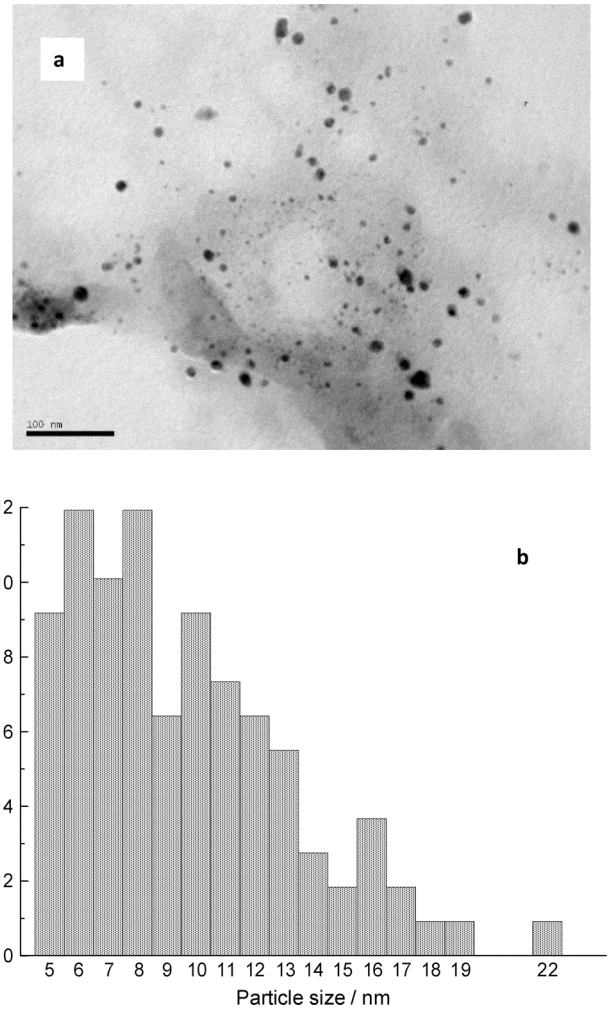

Fig. 2. TEM image taken from as prepared Ru-Co/BZY powder nanodispersed catalyst (a) and corresponding metal particle size distribution (b).

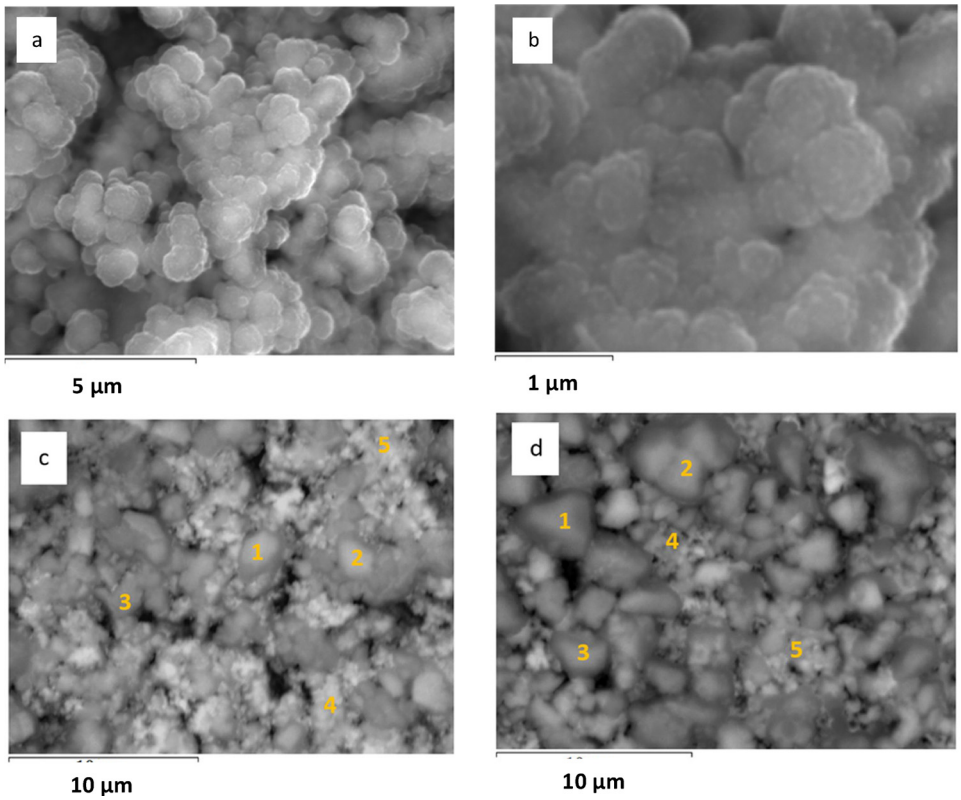

Fig. 3. SEM images of the catalyst surface before Ru-Co/BZY catalyst deposition (only with Ru film) (a) and (b), and after deposition of 0.5 mg/cm^2 (c) and 2.9 mg/cm^2 (d) dispersed catalyst respectively. Numbers indicate different compositions as discussed in the text.

2. Experimental

2.1. Catalyst preparation

The Ru-Co/BZY catalyst was prepared via the wet impregnation method using BZY powder as support and $Ru(NO_3)_2$ and $Co(NO_3)_2$ (Sigma Aldrich) as metal precursor salts. The resulting slurry was heated slowly at 65° under continuous stirring and maintained at that temperature until nearly all the water had evaporated. The solid residue was dried at 100 °C for 24 h and then reduced in H_2 flow at 450° for 1 h. The nominal Ru and Co loading of the catalyst was 2% and 15% respectively. The solid electrolytes were discs of BZY ($BaZr_{0.85}Y_{0.15}O_3$ + 1 w% NiO) with a diameter of 18 mm and a thickness of 2 mm (NorECs AS, Norway). Gold organometallic paste (Metalor, A1118) was used for the deposition of the Au counter and reference electrodes on one side of the disc, followed by calcination in air at 650 °C for 1 h. Blank experiments showed that gold was catalytically inactive both for methanation and the RWGS reaction. The Ru-Co/BZY dispersed catalyst was deposited on the other side of the solid electrolyte using a catalyst powder terpineol solution. Small amounts of the solution were added on a Ru film (previously deposited on the BZY disc) heated at 60 °C for 30 min and followed by calcination at 500 °C for 1h. A schematic drawing of the catalyst pellet is shown in Fig. 1. The interlayer Ru film (between the solid electrolyte and the dispersed catalyst) had a total mass of 2.1 mg and acted both as a catalyst and as a working electrode. It served both to enhance the adhesion between the catalyst and the solid electrolyte and also to increase the electronic conductivity of the electrode. Four different loadings of Ru-Co/BZY powder catalyst varying from 0.5 to 2.9 mg/cm^2 were deposited and studied. Prior to any hydrogenation activity measurements, a reduction pretreatment with H_2 (5% in He) was performed at 450 °C for 1 h.

The electrochemical promotion experiments were carried out in a continuous flow reactor, which has been thoroughly discussed previously [20,45]. The feed gas composition and total gas flow rate, F_v (200 cm^3/min) were controlled by a set of flow meters (Brooks smart mass flow and controller B5878). Reactants were certified standards of 5% CO_2 in He and 15% H_2 in He which were further diluted with pure (99.999%) He, in order to adjust the total flow rate and the inlet gas composition at desired levels. All the experiments were performed at ambient pressure. Reactants and products were analyzed by online gas chromatography (Shimadzu GC-2014) in conjunction with an IR CO_2-CO-CH_4 gas analyzer (Futzi Electric ZRE) and a Quadrapole Mass Spectrometer (Pfeiffer Omnistar). Constant currents and potentials were applied using an AMEL 2053 galvanostat- potentiostat.

2.2. Catalyst characterization

2.2.1. Ru-Co/BZY powder dispersed catalyst

The dispersed Ru-Co/BZY catalyst was characterized in terms of its dispersion by CO chemisorption at 298 K. The adsorption isotherms were obtained in the pressure range of 0–75 Torr employing a modified Fisons Instruments (Sorptomatic 1900) apparatus. Prior to each measurement, the catalyst sample (1 g) was pretreated by (a) exposure to vacuum at 523 K for 1 h; (b) reduction with 1 bar of H_2 at the same temperature for 1 h, (c) evacuation for 30 min, and (d) cooling down to the chemisorption temperature. After the first adsorption isotherm, the gas chamber was evacuated for 10 min followed by a second (reversible) adsorption in the same pressure range. The adsorption isotherms were extrapolated to zero pressure and the CO uptake at monolayer coverage was estimated by subtraction of the CO uptake of the reversible isotherm from the total amount of adsorbed CO. The exposed surface area of metal was calculated to be 1.8 m^2/g_{cat} (or 10.8 m^2/g_{met}) and the dispersion of the catalyst on the support was 1.7%. The adsorption isotherms together with the calculations are shown in detail in the supplementary material.

A JEOL JEM-2100 transmission electron microscope (TEM) was used to determine the mean metal particle size distribution and the morphology of the as prepared (without any reduction process) catalyst

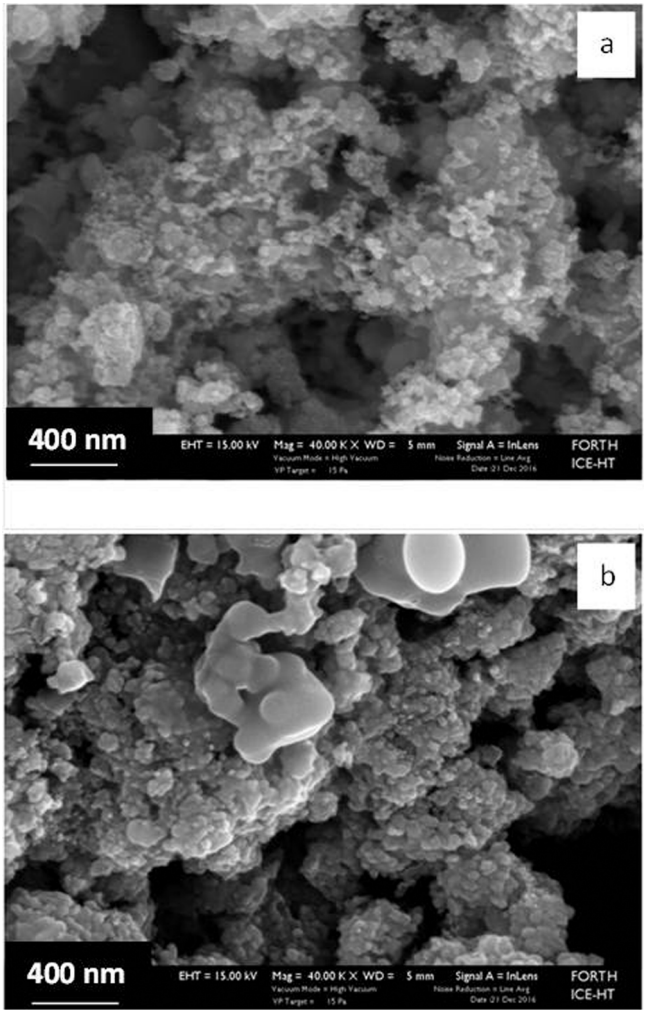

Fig. 4. SEM images of the catalytic surface before Ru-Co/BZY catalyst deposition (only with Ru film) (a) and after deposition of 0.5 mg/cm^2 (b).

(Ru-Co/BZY). Based on the TEM image shown in Fig. 2a, the particle size distribution of the metal particles shows both smaller (down to 5 nm) and bigger (up to 20 nm) particles with mean diameter 9.3 nm. Thus, it is clear that the prepared Ru-Co supported catalyst is a nano-dispersed catalyst. Analysis of the diffraction patterns of the TEM images (not shown here) shows three different diffraction rings corresponding to specific planes of barium zirconate ($BaZrO_3$), RuO_2 and CoO.

2.2.2. Ru and Ru-Co/Ru films deposited on BZY solid electrolyte

The morphology of the Ru and Ru-Co/Ru films deposited on BZY solid electrolyte was explored with scanning electron microscopy. SEM images were obtained with a JEOL 6300 microscope, equipped with an Oxford energy dispersive spectrometer (EDS). Higher magnifications were obtained using a Zeiss LEO SUPRA 35VP electron microscope without however ability for EDS analysis. Fig. 3 shows SEM images from the working electrode before Ru-Co/BZY deposition (i.e. only the Ru film, Fig. 3a and b) and after deposition of two different catalyst loadings (0.5 mg/cm^2, Fig. 3c and 2.9 mg/cm^2, Fig. 3d).

Due to the low magnification (limited by the microscope characteristics) of the images only particle aggregates were possible to be observed and no single particles. EDS analysis certified the existence of both Ru and Co on the surface (points 1, 2 and 3 in Fig. 3c and d). On the other hand, there are areas where the surface consists by pure Ru (points 4 and 5). The fraction of the surface which is covered by Ru-Co/BZY catalysts increases with catalyst loading (Fig. 3c and d). Fig. 5 shows higher magnification SEM images before (Fig. 4a) and after (Fig. 4b) deposition of 0.5 mg/cm^2 Ru-Co/BZY. The Ru film is uniform and porous with particles diameter varying from 10–30 nm (Fig. 4a). Addition of the dispersed catalyst powder results in bigger particles shown on the top side of Fig. 4b. The diameter of these particles (100–200 nm) is in agreement with the diameters observed by TEM (Fig. 2 in SP).

3. Results

3.1. Catalytic activity of the dispersed catalyst (Ru-Co/BZY)

Dispersed Ru-Co-BZY: In this case the catalyst is in a powder form placed in a fixed bed reactor. The RWGS reaction is favored due to the spontaneous thermal migration of protons from the support (BZY) to the metal particles (Ru and Co). Therefore, we refer to this catalyst as an already promoted one.

Initially we examined the catalytic activity of the dispersed Ru-Co/BZY catalyst powder in a fixed bed reactor between 250 °C and 450 °C. The feed partial pressures of H_2 and CO_2 were 7 kPa and 1 kPa respectively. The effect of temperature on the rates of the methanation and reverse water gas shift (RWGS) reactions is shown in Fig. 5.

Interestingly, the selectivity to CO is very high even at low temperatures while the selectivity to CH_4 is low and below 30%. This behavior is similar to the behavior of electrochemically promoted Ru films supported on proton solid electrolytes reported in previous papers [45,46]. In these cases, application of negative potential (proton supply to the catalytic surface) resulted in CO production enhancement (electrophilic behavior of the RWGS reaction). The activation energy for CH_4 and CO production based on Fig. 5 is 51 kJ/mol and 36 kJ/mol respectively, lower than most values reported in the literature for Ru and Co based catalysts [60–62]. However, according to more recent studies on CO_2 methanation [63–65] using Ru and/or Co based catalysts dispersed on various supports, the nature of the support plays a significant role on the catalytic activity, selectivity and activation energy for CH_4 production. Differences higher than 30 kJ/mol were reported [64] for the methanation reaction by changing the support from ZnO to CeO_2. We believe that the observed activation energies related strongly to the BZY support and further investigation is necessary.

Thus, the dispersed catalyst is somehow already in a promoted state for CO production, most probably due to the spontaneous thermal migration of protons from the support (BZY) to the metal particles (Ru and Co)

3.2. Catalytic activity and electropromotion of the Ru film

Unpromoted Ru-film-BZY: In this case the catalytic reaction takes place under open circuit conditions (without current or potential application). Thus, we have a catalytic reaction ($CO_2 + H_2$) on the Ru surface without any electrochemical reaction or the presence of any promoter.

Fig. 6 shows the effect of temperature on the selectivity to CH_4 and CO of the Ru film under open-circuit conditions, before Ru-Co/BZY deposition. The results are similar to previously reported data using Ru films on BZY solid electrolyte [45,46]. The clean and unpromoted Ru-film shows high selectivity to CH_4 at low temperatures and increased selectivity to CO as the temperature is increased. This behavior is in agreement with thermodynamics according to which the methanation reaction is favored at low temperatures and the RWGS reaction is favored at high temperatures. Based on Fig. 6, the activation energy for CH_4 and CO production is 64 kJ/mol and 98 kJ/mol. If we focus our attention on the RWGS reaction and compare the dispersed catalyst (Fig. 5) with the unpromoted Ru film (Fig. 6) it is obvious that CO production is pronounced and much easier in the first case probably due to the spontaneous thermal migration of protons from the support (BZY) to the metal particles (Ru and Co) which results in a decrease of

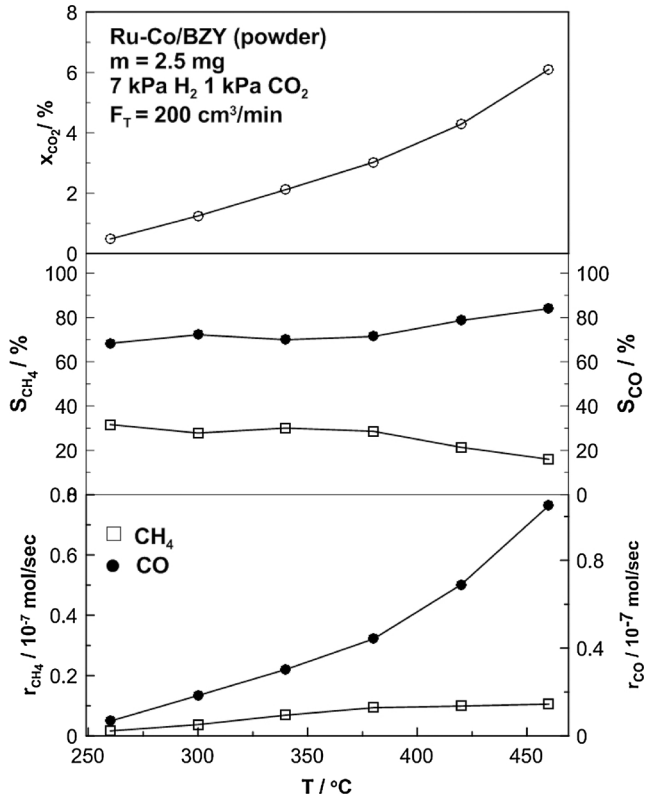

Fig. 5. Steady-state effect of temperature on the rates and selectivities to CH_4 and CO using 2.5 mg of Ru-Co/BZY dispersed catalyst in a fixed bed reactor. P_{H2} = 7 kPa, P_{CO2} = 1 kPa, F_T = 200 cm^3/min.

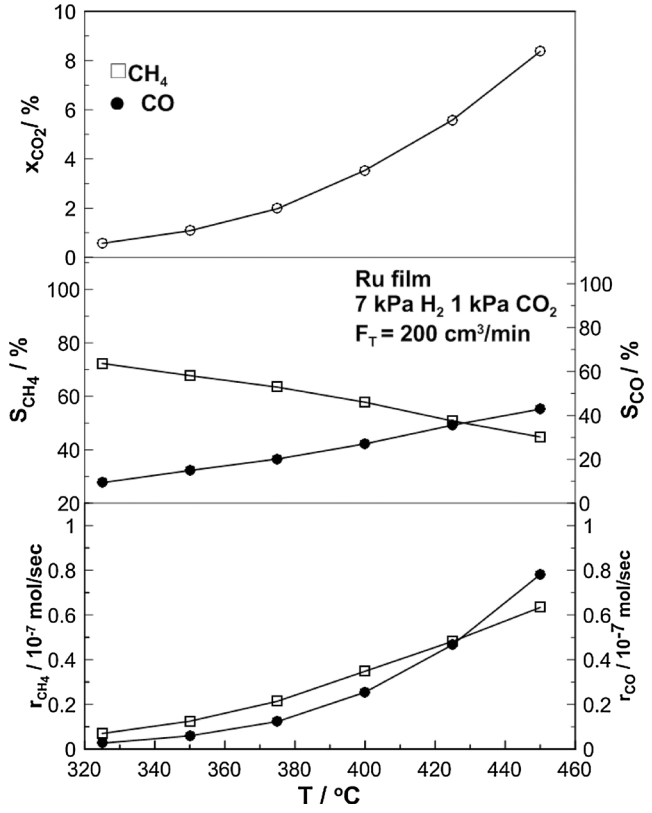

Fig. 6. Steady-state effect of temperature on the rates and the selectivities to CH_4 and CO on the Ru/BZY catalyst film. P_{H2} = 7 kPa, P_{CO2} = 1 kPa, F_T = 200 cm^3/min.

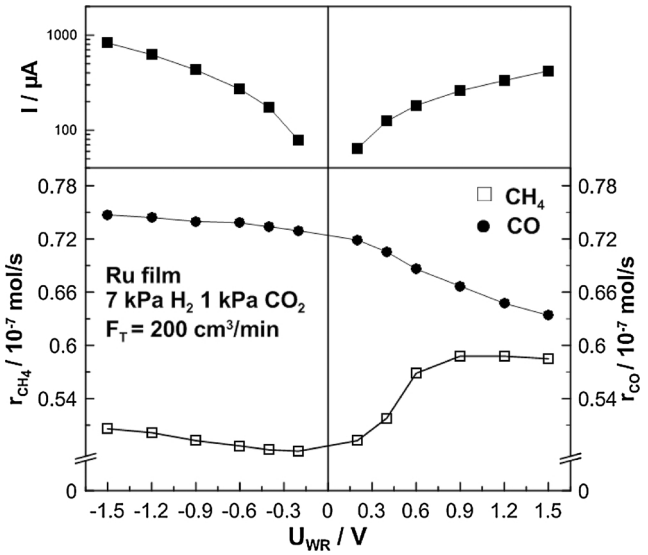

Fig. 7. Steady-state effect of catalyst potential, U_{WR}, on current and rates of CH_4 and CO formation on the Ru/BZY catalyst film. P_{H2} = 7 kPa, P_{CO2} = 1 kPa, T = 450 °C, F_T = 200 cm^3/min.

the catalyst work function and in a strengthening of the Ru-CO_x bond and weakening of the Ru-CO_x bond.

Promoted Ru-film-BZY: In this case the catalytic reaction takes place under closed circuit conditions (constant or potential application). Thus, we have a catalytic reaction ($CO_2 + H_2$) on the Ru surface together with the removal (or supply) of protons from (or to) the working electrode (catalyst) to (or from) the solid electrolyte via the electrochemical reaction: $(1/2)H_2(g) - e^- \rightarrow H^+(Ru) \rightarrow H^+(BZY)$. The presence of protons (under cathodic polarization) promotes the catalytic reaction of CO production (RWGS) while proton removal (under anodic polarization) enhances the methanation reaction.

Fig. 7 shows the effect of the catalyst potential on the CH_4 and CO production rates at a constant temperature of 450 °C. Although the methanation rate is initially much lower than the rate of CO production, the application of anodic polarization, i.e. proton removal from the catalyst surface according to the overall reaction (7)

$$(1/2)H_2(g) - e^- \rightarrow H^+(Ru) \rightarrow H^+(BZY) \quad (7)$$

results to an increase in the rate of CH_4 production and to a decrease in the rate of CO production.

The same trends are depicted also in the transients of Fig. 8 which present the transient effect of a constant applied positive (+1.5V) and negative (-1.5V) potential on the catalytic rates of CH_4 and CO formation. Proton removal from the catalyst surface causes an increase in the rate of methanation ($\rho_{CH_4} \approx 1.3$)and a decrease in the rate of CO formation ($\rho_{CO} \approx 0.8$). Both effects are reversible, i.e. the rates return to their initial values upon interruption of the applied potential. The corresponding Faradaic efficiencies are $\Lambda_{CH_4} = 28$ and $\Lambda_{CO} = -5.8$ respectively.

As also shown in Fig. 8, proton supply to the catalyst surface according to the reverse of Eq. (5) results to the opposite behavior (i.e. to an increase of CO production and a decrease of CH_4 production); however, the effect is here smaller. Similarly to recent studies of CO_2 hydrogenation on Ru using O^{2-}, Na^+ and K^+ solid electrolytes [42,46], the behavior is electrophobic (nucleophilic) for the methanation reaction ($\partial r_{CH_4}/\partial U_{WR} > 0$)and electrophilic ($\partial r_{CO}/\partial r_{WR} < 0$) for the reverse water gas shift (RWGS) reaction.

3.3. Catalytic activity and electropromotion of the dispersed (Ru-Co/BZY) catalyst

In this case the catalytic reaction takes place on an already

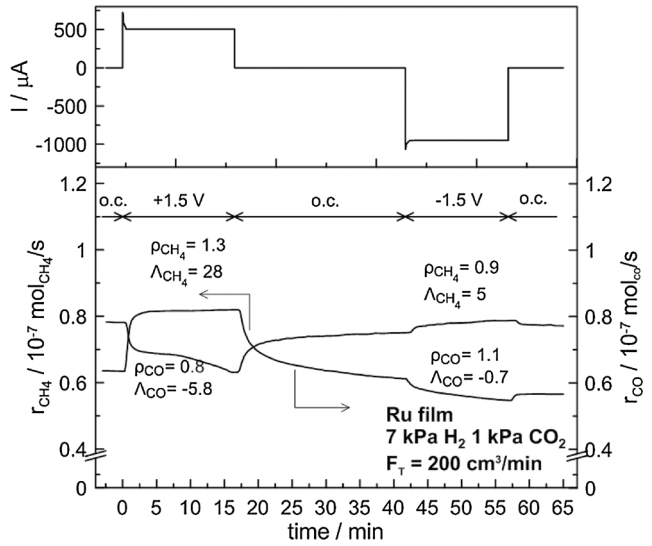

Fig. 8. Transient effect of constant applied positive (+1.5 V) and negative (−1.5 V) potential on the current and on the catalytic rates of CH_4 and CO formation on the Ru/BZY film. P_{H2} = 7 kPa, P_{CO2} = 1 kPa, T = 450 °C, F_T = 200 cm^3/min.

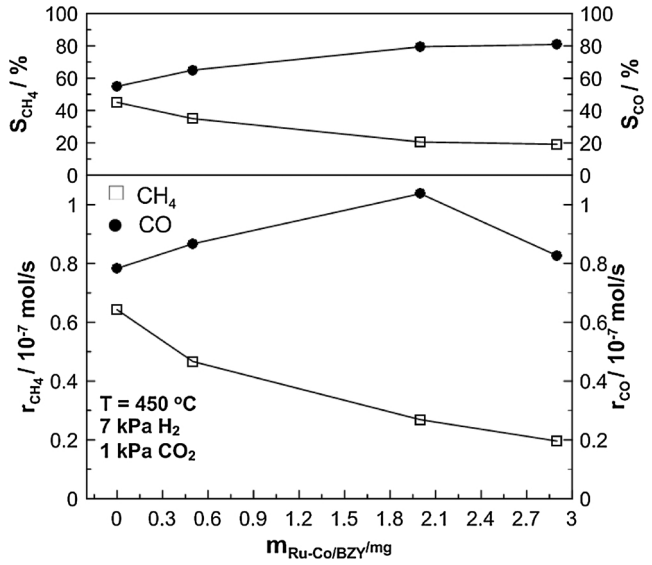

Fig. 9. Effect of dispersed Ru-Co/BZY catalyst loading on the rates and selectivities to CH_4 and CO at 450 °C. P_{H2} = 7 kPa, P_{CO2} = 1 kPa, T = 450 °C, F_T = 200 cm^3/min.

promoted catalyst (**dispersed Ru-Co-BZY**) which however has been deposited on a BZY solid electrolyte (with a Ru film interlayer). Using this configuration, we are able via anodic polarization to remove protons from the dispersed catalyst to the solid electrolyte and to promote the methanation reaction or to supply protons to the catalytic surface and promote the RWGS reaction.

Fig. 9 shows the effect of Ru-Co/BZY powder catalyst loading on the catalytic rates of CH_4 and CO formation together with the selectivity to the two products at zero applied current.

At zero loading ($m_{Ru\text{-}Co/BZY}$ = 0) the selectivity to CO is similar to that of CH_4. As the catalyst loading increases, the selectivity to CO rises up to 80% while the selectivity to CH_4 decreases to 20%. The increase of the RWGS reaction can be attributed to the catalytic contribution of the dispersed catalyst as shown in Fig. 5.

Fig. 10 shows the transient effect of a constant applied positive (+1.5 V) and negative (−1.5 V) potential on the catalytic rates of CH_4 and CO formation for the three different catalyst loadings at 450 °C. In all cases, the catalytic activity and selectivity of the dispersed catalyst

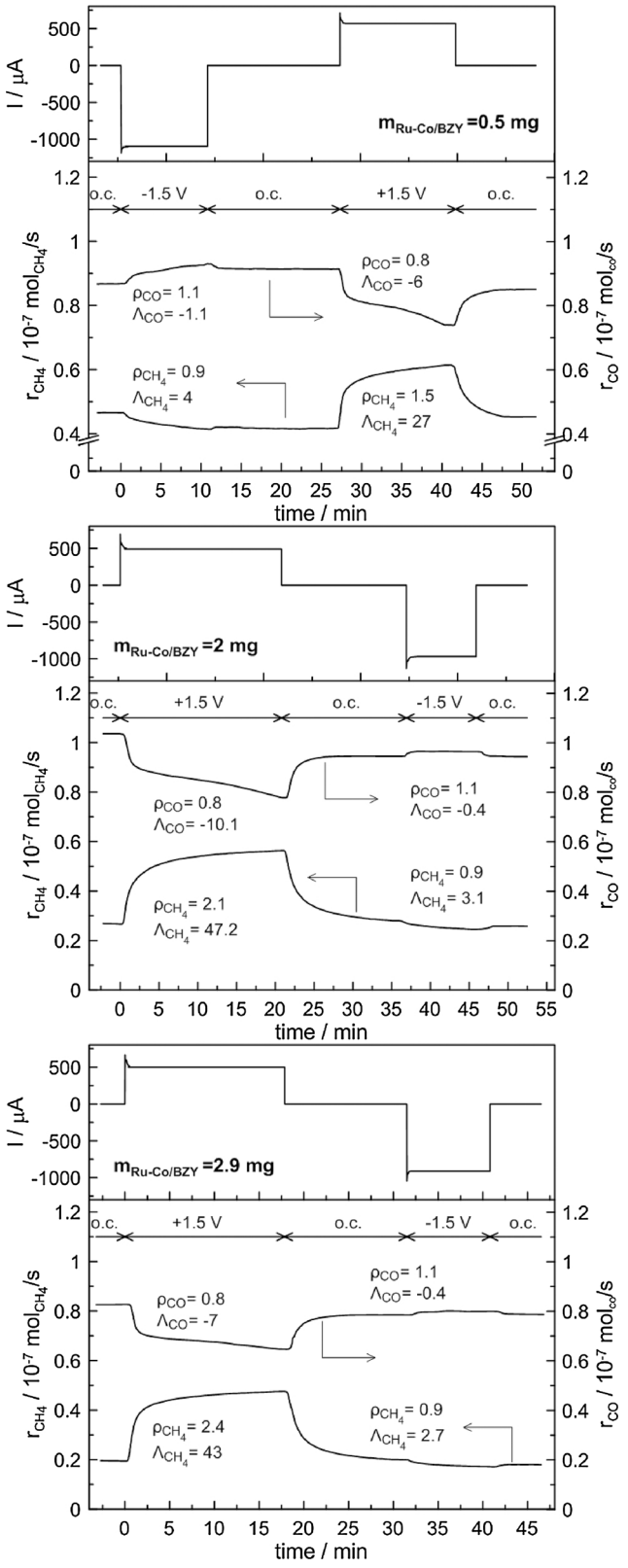

Fig. 10. Transient effect of constant applied positive (+1.5 V) and negative (−1.5 V) potential on the catalytic rates of CH_4 and CO formation and on the current for three different dispersed catalyst loadings. P_{H2} = 7 kPa, P_{CO2} = 1 kPa, T = 450 °C, F_T = 200 cm^3/min.

can be affected by proton supply or removal from the catalytic surface. Although the general behavior is always the same (electrophobic for the methanation and electrophilic for the RWGS) both the methane rate

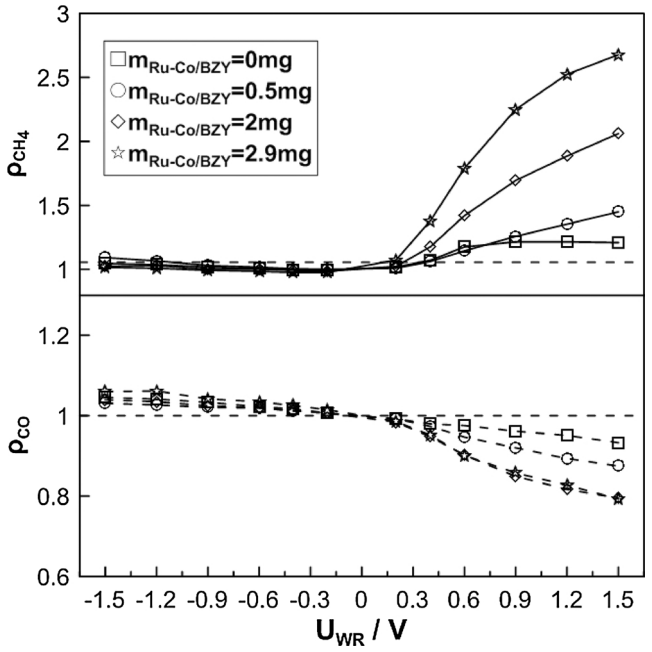

Fig. 11. Effect of dispersed Ru-Co/BZY catalyst loading and catalyst potential on the methane and CO production rate enhancement ratios. P_{H2} = 7 kPa, P_{CO2} = 1 kPa, T = 450 °C, F_T = 200 cm^3/min.

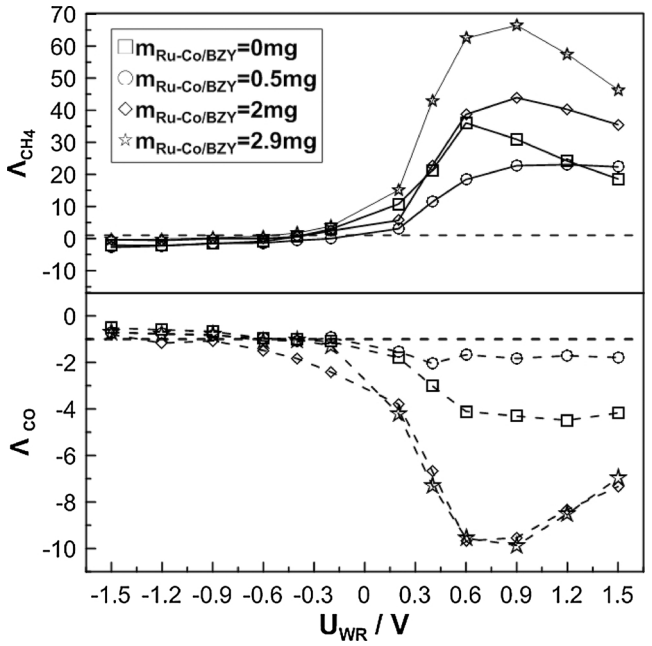

Fig. 12. Effect of dispersed Ru-Co/BZY catalyst loading and catalyst potential on the methane and CO production faradaic efficiencies. P_{H2} = 7 kPa, P_{CO2} = 1 kPa, T = 450 °C, F_T = 200 cm^3/min.

enhancement and the faradaic efficiency increase with dispersed catalyst loading (Fig. 11). This is shown more clearly in Figs. 12 and 10 which present the effect of potential on the ρ and Λ values both for CH_4 and CO production for all catalyst loadings. In general, the value of ρ decreases for CO and increases significantly for CH_4 as the catalyst potential increases. This behavior is more pronounced in the case of high catalyst loading.

Figs. 8 and 10 demonstrate that application of current or potential causes the rates of methanation and CO production to increase/decrease simultaneously and in opposite directions. This shows that the two reactions are parallel and not consecutive and demonstrates the

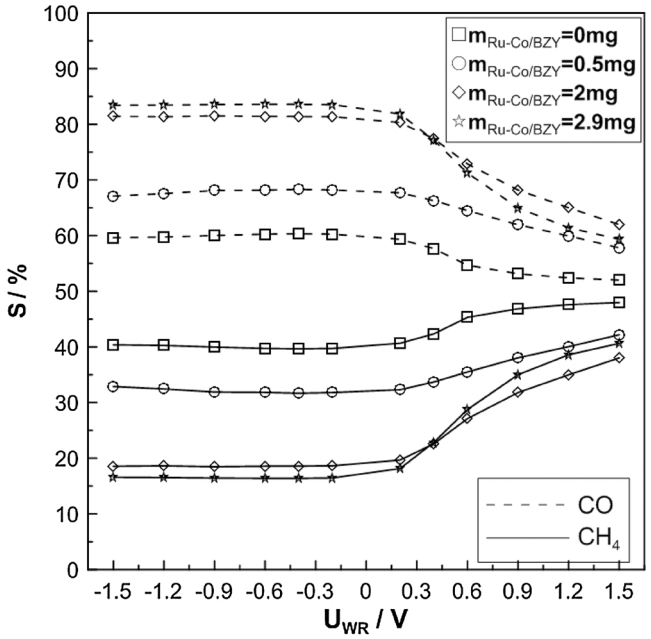

Fig. 13. Effect of catalyst potential and dispersed Ru-Co/BZY catalyst loading on the selectivity to CH_4 and CO. P_{H2} = 7 kPa, P_{CO2} = 1 kPa, T = 450 °C, F_T = 200 cm^3/min.

usefulness of EPOC for mechanistic investigations in heterogeneous catalysis.

Fig. 13 shows the selectivities to CH_4 and CO as a function of catalyst potential for all different catalyst loadings. It is clear that electrochemical promotion can affect significantly the selectivity of a dispersed catalyst. Thus the selectivity to CH_4 increases from 16% to 41% as the catalyst potential is varied between 0 and 1.5 V. Although the observed effect of catalyst loading on selectivity may indicate some structure sensitivity [66] of the present system, we believe that the main differences observed in the EPOC behavior are mainly due to the different loadings of the dispersed catalyst on the Ru film. The Ru nanoparticles dispersed on the BZY powder have a high selectivity to CO due to the easier transport of protons to their surface in comparison to the much larger surface of the film. Thus, as the catalyst loading on top of the Ru film increases, the production of CO (via the RWGS reaction) increases too and therefore the selectivity to CO is higher (Fig. 13). As a result, the effect of cathodic polarization (proton removal from the nanodispersed catalyst to the solid electrolyte) is more pronounced (Fig. 13).

4. Conclusions

The present results show that it is possible to electrochemically promote finely dispersed metal catalyst particles deposited on a solid electrolyte powder supported on a metal catalyst film which is in contact with a solid electrolyte disk and is being simultaneously electropromoted. This shows that electrochemically controlled spillover of promoting ions indeed takes place between the electrolyte disk and the surface of the nanoparticles. As a result, it appears that the same value of work function imposed, via potential application, to the metal film is also imposed to a large extent on the catalyst nanoparticles of the dispersed catalyst. This appears to create several interesting possibilities for the practical utilization of electrochemical promotion.

The present results also confirm the very close connection between metal-support interactions (MSI) and electrochemical promotion of Catalysis (EPOC). Thus, it is remarkable that Ru nanoparticles, but also films, deposited on BZY lead to high selectivity to CO, whereas similar Ru nanoparticles and films deposited on YSZ give high selectivities to CH_4 [42,46] Consequently the use of BZY corresponds to negative

applied potential (thus lower work function) of the catalyst, whereas the use of YSZ corresponds to positive applied potential (thus higher work function). These observations also clearly demonstrate the usefulness of EPOC for the optimal choice of catalyst supports.

Acknowledgements

The authors are thankful to the program “RESEARCH PROJECTS FOR EXCELLENCE IKY/SIEMENS” for financial support.

References

[1] W. Wang, S. Wang, X. Ma, J. Gong, Recent advances in catalytic hydrogenation of carbon dioxide, Chem. Soc. Rev. 40 (2011) 3703–3727.
[2] G. Centi, S. Perathoner, Perspectives and state of the art in producing solar fuels and chemicals from CO2, Green Carbon Dioxide, John Wiley & Sons, Inc., 2014, pp. 1–24.
[3] M.A.A. Aziz, A.A. Jalil, S. Triwahyono, A. Ahmad, CO2 methanation over heterogeneous catalysts: recent progress and future prospects, Green Chem. 17 (2015) 2647–2663.
[4] H.-R.M. Jhong, S. Ma, P.J. Kenis, Electrochemical conversion of CO2 to useful chemicals: current status, remaining challenges, and future opportunities, Curr. Opin. Chem. Eng. 2 (2013) 191–199.
[5] U. Rodemerck, M. Holeňa, E. Wagner, Q. Smejkal, A. Barkschat, M. Baerns, Catalyst development for CO2 hydrogenation to fuels, ChemCatChem 5 (2013) 1948–1955.
[6] A.L. Lapidus, N.A. Gaidai, N.V. Nekrasov, L.A. Tishkova, Y.A. Agafonov, T.N. Myshenkova, The mechanism of carbon dioxide hydrogenation on copper and nickel catalysts, Pet. Chem. 47 (2007) 75–82.
[7] R. Reske, M. Duca, M. Oezaslan, K.J.P. Schouten, M.T.M. Koper, P. Strasser, Controlling catalytic selectivities during CO2 electroreduction on thin Cu metal overlayers, J. Phys. Chem. Lett. 4 (2013) 2410–2413.
[8] M.R. Prairie, A. Renken, J.G. Highfield, K. Ravindranathan Thampi, M. Grätzel, A fourier transform infrared spectroscopic study of C02 methanation on supported ruthenium, J. Catal. 129 (1991) 130–144.
[9] W. Li, H. Wang, X. Jiang, J. Zhu, Z. Liu, X. Guo, C. Song, A short review of recent advances in CO2 hydrogenation to hydrocarbons over heterogeneous catalysts, RSC Adv. 8 (2018) 7651–7669.
[10] D. Li, N. Ichikuni, S. Shimazu, T. Uematsu, Catalytic properties of sprayed Ru/Al2O3 and promoter effects of alkali metals in CO2 hydrogenation, Appl. Catal. A 172 (1998) 351–358.
[11] B. Hu, C. Guild, S.L. Suib, Thermal, electrochemical, and photochemical conversion of CO_2 to fuels and value-added products, J. CO2 Util. 1 (2013) 18–27.
[12] C. Janke, M.S. Duyar, M. Hoskins, R. Farrauto, Catalytic and adsorption studies for the hydrogenation of CO2 to methane, Appl. Catal. B: Environ. 152–153 (2014) 184–191.
[13] S. Tada, O.J. Ochieng, R. Kikuchi, T. Haneda, H. Kameyama, Promotion of CO2 methanation activity and CH4 selectivity at low temperatures over Ru/CeO2/Al2O3 catalysts, Int. J. Hydrogen Energy 39 (2014) 10090–10100.
[14] M. Marwood, R. Doepper, A. Renken, In-situ surface and gas phase analysis for kinetic studies under transient conditions: the catalytic hydrogenation of CO2, Appl. Catal. A 151 (1997) 223–246.
[15] P. Panagiotopoulou, D.I. Kondarides, X.E. Verykios, Mechanistic study of the selective methanation of CO over Ru/TiO 2 catalyst: identification of active surface species and reaction pathways, J. Phys. Chem. C 115 (2011) 1220–1230.
[16] P. Panagiotopoulou, D.I. Kondarides, X.E. Verykios, Mechanistic aspects of the selective methanation of CO over Ru/TiO 2 catalyst, Catal. Today 181 (2012) 138–147.
[17] T.A. Le, M.S. Kim, S.H. Lee, E.D. Park, CO and CO2 methanation over supported cobalt catalysts, Top. Catal. 60 (2017) 714–720.
[18] R.E. Owen, P. Plucinski, D. Mattia, L. Torrente-Murciano, V.P. Ting, M.D. Jones, Effect of support of Co-Na-Mo catalysts on the direct conversion of CO2 to hydrocarbons, J. CO2 Util. 16 (2016) 97–103.
[19] H.H. Shin, L. Lu, Z. Yang, C.J. Kiely, S. McIntosh, Cobalt catalysts decorated with platinum atoms supported on barium zirconate provide enhanced activity and selectivity for CO2 methanation, ACS Catal. 6 (2016) 2811–2818.
[20] C.G. Vayenas, S. Bebelis, C. Pliangos, S. Brosda, D. Tsiplakides, Electrochemical Activation of Catalysis: Promotion, Electrochemical Promotion and Metal-Support Interactions, Kluwer Academic/Plenum Publishers, New York, 2001.
[21] C.G. Vayenas, C.G. Koutsodontis, Non-faradaic electrochemical activation of catalysis, J. Chem. Phys. 128 (2008) 182506.
[22] D. Tsiplakides, S. Balomenou, Milestones and perspectives in electrochemically promoted catalysis, Catal. Today 146 (2009) 312–318.
[23] C.G. Vayenas, Bridging electrochemistry and heterogeneous catalysis, J. Solid State Electrochem. 15 (2011) 1425–1435.
[24] A. Katsaounis, Recent developments and trends in the electrochemical promotion of catalysis (EPOC), J. Appl. Electrochem. 40 (2010) 885–902.
[25] P. Vernoux, L. Lizarraga, M.N. Tsampas, F.M. Sapountzi, A. De Lucas-Consuegra, J.-L. Valverde, S. Souentie, C.G. Vayenas, D. Tsiplakides, S. Balomenou, E.A. Baranova, Ionically conducting ceramics as active catalyst supports, Chem. Rev. 113 (2013) 8192–8260.
[26] M.N. Tsampas, F.M. Sapountzi, A. Boréave, P. Vernoux, Isotopical labeling mechanistic studies of electrochemical promotion of propane combustion on Pt/YSZ, Electrochem. Commun. 26 (2013) 13–16.
[27] S. Souentie, L. Lizarraga, A. Kambolis, M. Alves-Fortunato, J.L. Valverde, P. Vernoux, Electrochemical promotion of the water-gas shift reaction on Pt/YSZ, J. Catal. 283 (2011) 124–132.
[28] A. De Lucas-Consuegra, J. González-Cobos, Y. García-Rodríguez, A. Mosquera, J.L. Endrino, J.L. Valverde, Enhancing the catalytic activity and selectivity of the partial oxidation of methanol by electrochemical promotion, J. Catal. 293 (2012) 149–157.
[29] A. de Lucas-Consuegra, J. González-Cobos, V. Carcelén, C. Magén, J.L. Endrino, J.L. Valverde, Electrochemical promotion of Pt nanoparticles dispersed on a diamond-like carbon matrix: a novel electrocatalytic system for H2 production, J. Catal. 307 (2013) 18–26.
[30] M.A. Fortunato, A. Principalle, C. Capdeillayre, N. Petigny, C. Tardivat, C. Guizard, M.N. Tsampas, F.M. Sapountzi, P. Vernoux, Role of lattice oxygen in the propane combustion over Pt/Yttria-stabilized zirconia : isotopic studies, Top. Catal. 57 (2014) 1277–1286.
[31] C.G. Vayenas, S. Bebelis, S. Ladas, Dependence of catalytic rates on catalyst work function, Nature 343 (1990) 625–627.
[32] C.G. Vayenas, S. Bebelis, I.V. Yentekakis, P. Tsiakaras, H. Karasali, Non-faradaic electrochemical modification of catalytic activity reversible promotion of platinum metals catalysts, Platinum Met. Rev. 34 (1990) 122–130.
[33] H.-G. Lintz, C.G. Vayenas, Solid ion conductors in heterogeneous catalysis, Angew. Chem. – Int. Ed. Engl. 28 (1989) 708–715.
[34] M. Stoukides, C.G. Vayenas, Electrocatalytic rate enhancement of propylene epoxidation on porous silver electrodes using a zirconia oxygen pump, J. Electrochem. Soc. 131 (1984) 839–845.
[35] G. Pacchioni, F. Illas, S.G. Neophytides, C.G. Vayenas, Quantum-chemical study of electrochemical promotion in catalysis, J. Phys. Chem. 100 (1996) 16653–16661.
[36] A. Katsaounis, Z. Nikopoulou, X.E. Verykios, C.G. Vayenas, Comparative isotope-aided investigation of electrochemical promotion and metal–support interactions 1. 18O2 TPD of electropromoted Pt films deposited on YSZ and of dispersed Pt/YSZ catalysts, J. Catal. 222 (2004) 192–206.
[37] A. Katsaounis, Z. Nikopoulou, X.E. Verykios, C.G. Vayenas, Comparative isotope-aided investigation of electrochemical promotion and metal-support interactions: 2. CO oxidation by 18O2 on electropromoted Pt films deposited on YSZ and on nanodispersed Pt/YSZ catalysts, J. Catal. 226 (2004) 197–209.
[38] C.G. Vayenas, S. Brosda, C. Pliangos, Rules and mathematical modeling of electrochemical and chemical promotion: 1. Reaction classification and promotional rules, J. Catal. 203 (2001) 329–350.
[39] J. Fleig, J. Jamnik, Work function changes of polarized electrodes on solid electrolytes, J. Electrochem. Soc. 152 (2005) E138–E145.
[40] S. Brosda, C.G. Vayenas, J. Wei, Rules of chemical promotion, Appl. Catal. B: Environ. 68 (2006) 109–124.
[41] C. Vayenas, S. Brosda, Electron donation–backdonation and the rules of catalytic promotion, Top. Catal 57 (2014) 1287–1301.
[42] D. Theleritis, S. Souentie, A. Siokou, A. Katsaounis, C.G. Vayenas, Hydrogenation of CO2 over Ru/YSZ electropromoted catalysts, ACS Catal. 2 (2012) 770–780.
[43] D. Theleritis, M. Makri, S. Souentie, A. Caravaca, A. Katsaounis, C.G. Vayenas, Comparative study of the electrochemical promotion of CO2 hydrogenation over Ru-supported catalysts using electronegative and electropositive promoters, ChemCatChem 1 (2014) 254–262.
[44] M. Makri, A. Katsaounis, C.G. Vayenas, Electrochemical promotion of CO2 hydrogenation on Ru catalyst–electrodes supported on a K–β″–Al2O3 solid electrolyte, Electrochim. Acta 179 (2015) 556–564.
[45] I. Kalaitzidou, A. Katsaounis, T. Norby, C.G. Vayenas, Electrochemical promotion of the hydrogenation of CO2 on Ru deposited on a BZY proton conductor, J. Catal. 331 (2015) 98–109.
[46] I. Kalaitzidou, M. Makri, D. Theleritis, A. Katsaounis, C.G. Vayenas, Comparative study of the electrochemical promotion of CO2 hydrogenation on Ru using Na^{++}, K^{++}, H^{++} and O^{2-} conducting solid electrolytes, Surf. Sci. 646 (2016) 194–203.
[47] A. Kambolis, L. Lizarraga, M.N. Tsampas, L. Burel, M. Rieu, J.P. Viricelle, P. Vernoux, Electrochemical promotion of catalysis with highly dispersed Pt nanoparticles, Electrochem. Commun. 19 (2012) 5–8.
[48] C.G. Yiokari, G.E. Pitselis, D.G. Polydoros, A.D. Katsaounis, C.G. Vayenas, High-pressure electrochemical promotion of ammonia synthesis over an industrial iron catalyst, J. Phys. Chem. A 104 (2000) 10600–10602.
[49] Z. Wang, H. Huang, H. Liu, X. Zhou, Self-sustained electrochemical promotion catalysts for partial oxidation reforming of heavy hydrocarbons, Int. J. Hydrogen Energy 37 (2012) 17928–17935.
[50] X. Zhou, H. Huang, H. Liu, Study of partial oxidation reforming of methane to syngas over self-sustained electrochemical promotion catalyst, Int. J. Hydrogen Energy 38 (2013) 6391–6396.
[51] J. Nicole, D. Tsiplakides, C. Pliangos, X.E. Verykios, C. Comninellis, C.G. Vayenas, Electrochemical promotion and metal-support interactions, J. Catal. 204 (2001) 23–34.
[52] I. Constantinou, D. Archonta, S. Brosda, M. Lepage, Y. Sakamoto, C.G. Vayenas, Electrochemical promotion of NO reduction by C3H6 on Rh catalyst-electrode films supported on YSZ and on dispersed Rh/YSZ catalysts, J. Catal. 251 (2007) 400–409.
[53] Y.M. Hajar, K.D. Patel, U. Tariq, E.A. Baranova, Functional equivalence of electrochemical promotion and metal support interaction for Pt and RuO2 nanoparticles, J. Catal. 352 (2017) 42–51.
[54] K.D. Kreuer, Proton conductivity: materials and applications, Chem. Mater. 8 (1996) 610–641.
[55] T. Norby, Solid-state protonic conductors: principles, properties, progress and prospects, Solid State Ionics 125 (1999) 1–11.

[56] A. Goñi-Urtiaga, D. Presvytes, K. Scott, Solid acids as electrolyte materials for proton exchange membrane (PEM) electrolysis: review, Int. J. Hydrogen Energy 37 (2012) 3358–3372.
[57] J. Lyagaeva, N. Danilov, D. Korona, A. Farlenkov, D. Medvedev, A. Demin, I. Animitsa, P. Tsiakaras, Improved ceramic and electrical properties of CaZrO3-based proton-conducting materials prepared by a new convenient combustion synthesis method, Ceram. Int. 43 (2017) 7184–7192.
[58] D. Medvedev, J. Lyagaeva, G. Vdovin, S. Beresnev, A. Demin, P. Tsiakaras, A tape calendering method as an effective way for the preparation of proton ceramic fuel cells with enhanced performance, Electrochim. Acta 210 (2016) 681–688.
[59] D.A. Medvedev, J.G. Lyagaeva, E.V. Gorbova, A.K. Demin, P. Tsiakaras, Advanced materials for SOFC application: strategies for the development of highly conductive and stable solid oxide proton electrolytes, Prog. Mater Sci. 75 (2016) 38–79.
[60] K. Müller, M. Städter, F. Rachow, D. Hoffmannbeck, D. Schmeißer, Sabatier-based CO2-methanation by catalytic conversion, Environ. Earth Sci. 70 (2013) 3771–3778.
[61] G.D. Weatherbee, C.H. Bartholomew, Hydrogenation of CO2 on group VIII metals. IV. Specific activities and selectivities of silica-supported Co, Fe, and Ru, J. Catal. 87 (1984) 352–362.
[62] F. Solymosi, A. Erdöhelyi, Hydrogenation of CO2 to CH4 over alumina-supported noble metals, J. Mol. Catal. 8 (1980) 471–474.
[63] J. Díez-Ramírez, P. Sánchez, V. Kyriakou, S. Zafeiratos, G.E. Marnellos, M. Konsolakis, F. Dorado, Effect of support nature on the cobalt-catalyzed CO2 hydrogenation, J. CO2 Util. 21 (2017) 562–571.
[64] J.A.H. Dreyer, P. Li, L. Zhang, G.K. Beh, R. Zhang, P.H.L. Sit, W.Y. Teoh, Influence of the oxide support reducibility on the CO2 methanation over Ru-based catalysts, Appl. Catal. B: Environ. 219 (2017) 715–726.
[65] J. Dou, Y. Sheng, C. Choong, L. Chen, H.C. Zeng, Silica nanowires encapsulated Ru nanoparticles as stable nanocatalysts for selective hydrogenation of CO2 to CO, Appl. Catal. B: Environ. 219 (2017) 580–591.
[66] M.C. Román-Martínez, D. Cazorla-Amorós, C. Salinas-Martínez de Lecea, A. Linares-Solano, Structure sensitivity of CO2 hydrogenation reaction catalyzed by Pt/carbon catalysts, Langmuir 12 (1996) 379–385.